Green Chemistry

Accepted Manuscript

This article can be cited before page numbers have been issued, to do this please use: X. Sun, Q. Zhu, X. Kang, H. Liu, Q. Qian, J. Ma, Z. Zhang, G. Yang and B. Han, *Green Chem.*, 2017, DOI: 10.1039/C7GC00503B.

ROYAL SOCIETY OF CHEMISTRY

rsc.li/green-chem

View Article Online
DOI: 10.1039/C7GC00503B

Journal Name

ARTICLE

Design of Cu (I)/C-doped boron nitride electrocatalyst for efficient conversion of CO_2 into acetic acid

Received 00th January 20xx,
Accepted 00th January 20xx

DOI: 10.1039/x0xx00000x

www.rsc.org/

Xiaofu Sun,[a,b] Qinggong Zhu,[a] Xinchen Kang,[a,b] Huizhen Liu,[a,b] Qingli Qian,[a] Jun Ma,[a] Zhaofu Zhang,[a] Guanying Yang,[a] and Buxing Han*[a,b]

Electrocatalytic CO_2 reduction to C_2 products is a promising technique when compared with the traditionally complicated and energy intensive routes in the industrial process. As an important bulk chemical, acetic acid is highly desirable for producing *via* sustainable method. In this work, we prepared N-based Cu (I)/C-doped boron nitride (BN-C) composites for electrocatalytic reduction of CO_2 to acetic acid. It was found that the Faradaic efficiency of acetic acid could reach as high as 80.3 % with a current density of 13.9 mA cm^{-2} when 1-ethyl-3-methylimidazolium tetrafluoroborate ([Emim]BF_4)-LiI-water solution was used as the electrolyte, which was about 4 times higher than the best value reported in the literature. Detailed study further indicated that Cu complex, BN-C, and the electrolyte have excellent synergistic effect for producing acetic acid. Especially, as a promoter, LiI played a key role for the C-C coupling to form acetic acid in the electrocatalytic process. Our study shows a promising way for producing C_2 product *via* electrochemical reduction of CO_2 by combination of composite electrodes and electrolytes with a promoter.

Introduction

The demand of fossil resource is increasing for energy and chemicals. [1,2] However, fossil resource is not renewable and the reserve is limited. CO_2 is nontoxic, cheap and abundant carbon resource. Developing efficient methods for the conversion of CO_2 to value-added chemical products are of technological and societal importance. [3-6] In the past two decades, electrocatalytic CO_2 reduction has attracted increasing attention because the required electricity may be obtained from renewable energy sources, such as wind, wave and solar. [7-9] In most cases, the products from electrochemical reduction processes can be tuned by varying reaction conditions at ambient temperature and pressure. Exploration of efficient and selective catalysts and electrolytes are crucial for electrocatalytic CO_2 reduction.[8] Particularly, converting CO_2 to C_2 products is much more attractive because synthesis of C_2 products is more complicated and energy intensive in the current industrial processes.[10,11] However, the mild electrocatalytic reduction of CO_2 to C_2 products is challenging because C-C coupling is very difficult in electrocatalytic reduction.

Cu-based materials were found to be the most promising electrocatalysts for converting CO_2 to C_2+ products. [12-18] Many efforts have been devoted to tuning the composition and structure of Cu-based materials with the aim of optimizing the C_2 selectivity. Cu nanotube and Cu_2O films exhibited high selectivity for transforming CO_2 to ethylene. [12-14] Ethanol and ethane were also formed on Cu_2O films. [12,14] Bouwman*et al.* reported that a dinuclear Cu (I) complex could be used as a catalyst for the reductive coupling of CO_2 to oxalate upon electrochemical reduction. [15] Lee *et al.* demonstrated a Cl-induced bi-phasic Cu_2O-Cu catalyst for the formation of C_3-C_4 compounds. [16] Mechanism of Cu-catalyzed reduction of CO_2 to C_2+ products has also been studied. [10,17,18] It was also reported that N-based organometallic catalysts could enhance the efficiency of electrochemical reduction CO_2 by reducing the overpotential and increasing the product selectively. [8] N-doped materials or N-containing ligands have higher overpotential for hydrogen evolution which may inhibit H_2O reduction, and thus enhancing the selectivity to desired product.[8,9] Besides, they have excellent chemical stability to keep high active in long-term operation. [19-21] In addition, N species, especially pyridinic and pyridonic/pyrrolic N, can act as electrochemically active species for the adsorption of CO_2 and $CO_2^{\cdot-}$. [22,23]

Boron nitride (BN) has been found to be composed of alternating B and N atoms in a honeycomb arrangement consisting of sp^2-bonded 2D layers, which has a similar structural lattice as that of the C atoms of graphene. [24] Their unique properties, such as high thermal conductivity, mechanical properties and high resistance to oxidation, make them very promising in many potential applications, especially in optoelectronic nanodevices, electro-/photo-catalysts, functional composites, etc. [24] Recent investigations indicated that BNs had the ability to produce CO_2 chemisorption once an

[a] Beijing National Laboratory for Molecular Sciences, Key Laboratory of Colloid and Interface and Thermodynamics, Institute of Chemistry, Chinese Academy of Sciences, Beijing 100190, P.R.China, E-mail: hanbx@iccas.ac.cn
[b] University of Chinese Academy of Sciences, Beijing 100049, P.R.China

Electronic Supplementary Information (ESI) available: [Details of the experimental procedures and other figures and tables]. See DOI: 10.1039/x0xx00000x

View Article Online
DOI: 10.1039/C7GC00503B

extra electron is injected into the material.[25-27] CO_2 reduction based on BN-like materials may be possible.

Acetic acid is an important petrochemical that is currently synthesized in an energy-intensive process using methane or coal as the feedstocks.[28,29] Efficient synthesis of acetic acid *via* electrocatalytic CO_2 reduction is very attractive, but is challenging. Also, LiI is a common promoter in organic reaction.[29] The proper ion size and stronger Lewis acidity of Li^+ as well as the strong nucleophilicity of I^- would facilitate the C-C bond formation. Therefore, the combination of BN-like materials support, N-based Cu (I) catalysts, and electrolytes with a promoter (LiI) may be an effective way to solve the challenging problem.

In this work, we synthesized Cu (I) complex/BN-C_x composites, in which Cu (I) complex was supported on C-doped BN. The materials were used as electrocatalyst for CO_2 reduction to acetic acid. It was discovered that the Faradaic efficiency of acetic acid could reach 80.3 % at a current density of 13.9 mA cm^{-2} when [Emim]BF_4-LiI-water solution was used as the electrolyte, which presents the best result reported up to date.

Results and discussion

Electronic supplementary information (ESI) provides details regarding catalyst synthesis. Scheme S1 shows molecular structures of the ligands and Cu complexes.[30-32] For clarity, **Cu 1** and **Cu 2** refer to complexes with the ligands of N,N,N',N'-tetra(2-pyridyl)-2,6-pyridinediamine (Tppda) and N,N,N',N'-tetra(2-pyridyl)-biphenyl-4,4'-diamine (Tpbpa), respectively. BN-C_x refers to C-doped BN support, where x is the weight percentage of glucose (C precursor) of the boron oxide (B precursor) used in the BN-C_x synthesis.

Fig. 1, S1-S6 and Tables S1-S2 show the structure characterization of the BN-C_x. Fig. 1A depicts thescanning electron microscopy (SEM) image of BN-C_{30}. The material has the sheet structure with a size thickness of about 60 nm. High-resolution transmission electron microscopy (HR-TEM) image (Fig. 1B) confirms that an interlayer crystal lattice spacing of 0.33 nm exists in the nanosheet. Elemental distribution mappings (Fig. 1C) further show uniform distribution of B, N and C in the materials, indicating homogeneity of the C-doped BN ternary materials. X-ray photoelectron spectroscopy (XPS) spectra (Fig. 1D and Fig. S1) show the chemical nature of the BN-C_{30}, including the peaks belonging to B1s (B-N: 190.4 eV; B-C: 190.0 eV; B-O: 192.2 eV), N1s (N-B: 397.7 eV; N-C: 399.2 eV), and C1s (C-C: 283.9 eV; C-N: 285.5 eV; C-B: 283.0 eV).[33] We can also found that the C content of BN-C_x increased with increasing glucose amount gradually (Table S2). These provide direct evidence that the incorporation of C into BN. Fig. 1E shows the X-ray diffraction (XRD) pattern of the BN-C_{30}. Two characteristic peaks at 26.4° and 42.2° can be attributed to the (002) and (100) planes of graphitic structure of BN, respectively.[34] ^{13}C resonance appears around 125 ppm in the ^{13}C solid-state NMR spectrum (Fig. 1F), which corresponds to sp^2C atoms with an electron density very similar to reduced graphene oxide/graphite.[33] The detailed characterizations of the BN-C_x with different glucose contents are shown in the ESI (Figs. S2-S6), which indicate that the BN-C_x nanosheets had similar structures to that of BN-C_{30}. **Cu 1** and **Cu 2** supported on BN-C_x were synthesized. The catalysts were suspended in acetone with Nafion D-521 dispersion (5 wt%) to form a homogeneous ink assisted by ultrasound and spread onto the carbon paper (CP) surface to obtain the working electrodes.

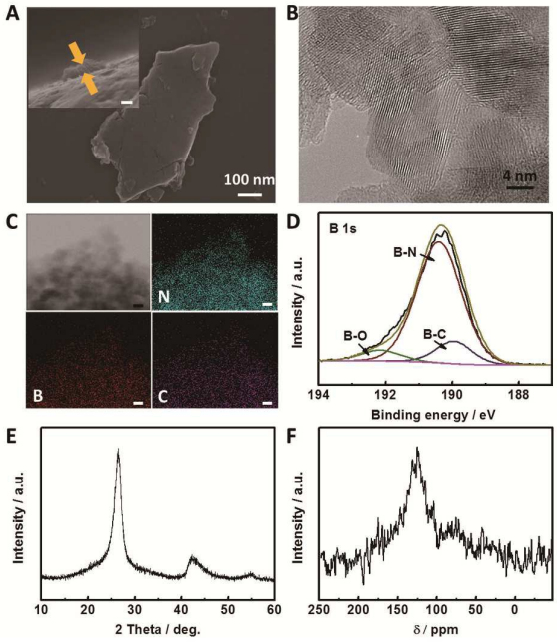

Fig. 1 A) SEM image of BN-C_{30}. Inset of A shows the thickness of the BN-C_{30} (scale bar, 50 nm). **B)** HR-TEM image of BN-C_{30}. **C)** Elemental mappings of BN-C_{30} (scale bar, 10 nm). **D)** XPS spectrum of B 1s orbit of BN-C_{30}. **E)** Powder XRD pattern of BN-C_{30}. **F)** ^{13}C solid-state NMR spectrum of BN-C_{30}.

The performance of the as-prepared electrodes for electrocatalytic CO_2 reduction was first examined in CO_2 or N_2 saturated [Emim]BF_4 aqueous solution with 25 mol% [Emim]BF_4 in the presence of 0.01 M LiI by linear sweep voltammetry (LSV). As shown in Fig. S7, obvious reduction peaks are observed for both **Cu 1**/BN-C_{30} and **Cu 2**/BN-C_{30} electrodes. The much higher current density of the CO_2-saturated system than the N_2-saturated system indicates the reduction of CO_2.

Based on the above results, controlled potential electrolysis of CO_2 was performed at different applied potentials between -1.7 V and -2.4 V vs Ag/Ag^+ in CO_2 saturated [Emim]BF_4 aqueous solution with 25 mol% [Emim]BF_4 containing 0.01 M LiI to test the catalytic activity of the synthesized catalysts, and a typical H-type cell was used.[23] Under the reported reaction conditions, acetic acid, formic acid and methanol were the liquid products detected by NMR spectroscopy, and H_2 was the only gaseous product determined by gas chromatography (GC). The Faradaic efficiency was calculated from moles of each product and total number of electrons and the details can be seen in the ESI.[9,12]

View Article Online
DOI: 10.1039/C7GC00503B

Fig. 2A and 2B show the current density and Faradaic efficiency for each product over **Cu 1**/BN-C_{30} and **Cu 2**/BN-C_{30} electrodes at different applied potentials. CO_2 reduction occurred with the increasing applied potential, and formic acid and methanol were produced at low potentials, and acetic acid was generated at higher potentials. The highest Faradaic efficiency of acetic acid occurred at -2.2 V vs Ag/Ag^+ and the performance of **Cu 1**/BN-C_{30} electrode was much better than **Cu 2**/BN-C_{30} electrode. If we change the potential with respect to reversible hydrogen electrode (RHE), the potential was about -1.3 V vs RHE. The Faradaic efficiency of acetic acid could reach 80.3 % over **Cu 1**/BN-C_{30} electrode with a current density of 13.9 mA cm^{-2}, which is about 4 times higher than the best result reported to date at the similar Faradaic efficiency (Table S3). The competitive hydrogen evolution reaction (HER) became much higher above -2.2 V vs Ag/Ag^+, leading to the decreasing of Faradaic efficiency of acetic acid. We conducted the blank experiment at -2.2 V vs Ag/Ag^+, in which N_2 was used to replace CO_2. The current density was nearly zero (Fig. S7). ^1H NMR spectra (Fig. S8) showed that there was no liquid product, indicating that the CO_2 was the carbon source for the product. To further verify that the liquid product was derived from CO_2 reduction, isotope-labeled $^{13}CO_2$ was used to study the reaction over **Cu 1**/BN-C_{30} electrode at -2.2 V vs Ag/Ag^+. ^1H NMR spectra (Fig. S9A-9C) indicated that only ^{13}C signal was observed for the product, demonstrating that the acetic acid was derived from CO_2 rather than other organic chemicals in the reaction system. The splitting of H peaks of formic acid, methanol and acetic acid by the ^{13}C atom with relatively large coupling constants can be observed. They are not the single peaks. They distributes on both sides of the chemical shift of H-^{12}C symmetrically. To further confirm that the acetic acid was derived from CO_2, we also characterized the product by ^{13}C NMR，and the results are given in the ESI (Fig. S9D). The results showed that no C signal attributed to acetic acid, formic acid and methanol can be found when $^{12}CO_2$ was used as the feedstock, but strong C signal can be seen as $^{13}CO_2$ was used. Thus, the blank experiment using N_2 (no product), as well as ^1H NMR and ^{13}C NMR characterizations of the product using $^{12}CO_2$ and $^{13}CO_2$ all showed that the product was only derived from CO_2.

The electrode stability was also tested with an electrolysis time of 5 h (Fig. S10), and the current density did not change obviously with time. We tried to dissolve **Cu 1**/BN-C_{30} after electrolysis of into dichloromethane with the aid of ultrasound. Both the ligand Tppda and **Cu 1** complex exhibit photoluminescence in the solid state. The emission spectra of them are shown in Fig. S11. The individual ligand exhibits strong emission band in the 350-475 nm region (λ_{max} = 401 nm) upon excitation with λ_{max} = 276 nm. It is due to the $\pi \rightarrow \pi^*$ transition.[31] After the ligand coordinates to Cu^{1+}, a significant red shift of the emission peak (λ_{max} = 526 nm) can be observed. The emission bands of **Cu 1** complex before and after electrolysis were the same, indicating that **Cu 1** was stable during the CO_2 reduction. We did parallel experiments to recover the complex from the used electrodes (after electrolysis) and virgin electrodes (before used) by repeating 5 times, and percentages of the complex recovered from the used electrode and virgin electrode were 75.8 ± 1.6% and 76.7 ± 2.0%, respectively. The values were the same in the experimental error range. There were mainly two reasons for that 25% could not be recovered from the electrodes. First, it is impossible to remove all complex from CP due to the adsorption; second, only about 0.12 mg complex was used for each electrode, and thus little loss covers large percentage. Besides, after electrolysis the electrolyte was characterized NMR method, and the spectrum was the same as that of the original electrolyte. The excellent long-term stability of the electrode during electrolysis (Fig S10), the emission spectra of the complex before and after electrolysis (Fig S11), the results of recovery experiments for the complex from the electrodes, and the NMR characterization of the electrolyte before and after electrolysis all showed that the complex in the electrode and the electrolyte were stable during the electrolysis. For comparison, the aqueous solutions of some other typical supporting electrolytes were also used, but their performances were not as good as $[Emim]BF_4$ (Table S4).

The role of BN-C_x support in the electrolysis was also investigated. Very little amount of acetic acid was formed when **Cu 1**/C and **Cu 2**/C as electrodes (Fig. S12). When BN-C_x was used separately, the main product was formic acid (Fig. S13). There was no CO_2 reduction product when bulk BN was used. Obviously, synergistic effect existed between Cu complexes and BN-C_x in promoting CO_2 reduction to acetic acid. We also combined **Cu 1** and **Cu 2** with other BN-C_x, and BN-C_{30} gave the best results (Fig. S14-S16).

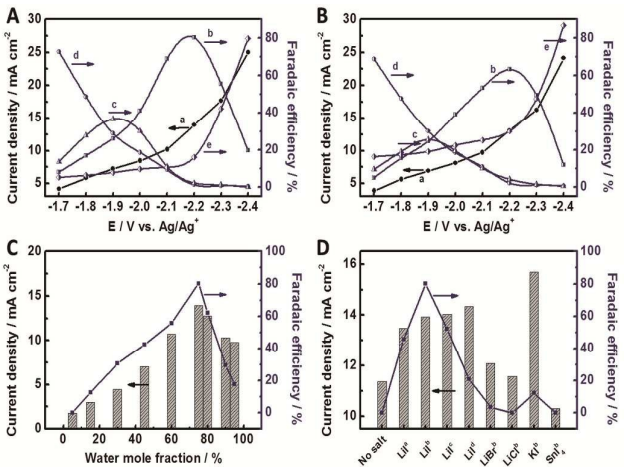

Fig. 2 Current density and Faradaic efficiency of the products at different applied potentials over (**A**) **Cu 1**/BN-C_{30} and (**B**) **Cu 2**/BN-C_{30} electrodes in aqueous solution of 25 mol% $[Emim]BF_4$ and 75 mol% water in the presence of 0.01 M LiI at 1 atm CO_2 and room temperature with 5 h electrolysis. Curve (a) is the current density; curves (b)-(e) are Faradaic efficiency of b) acetic acid, c) methanol, d) formic acid, and e) H_2. Current density and Faradaic efficiency of acetic acid at applied potential of -2.2 V vs Ag/Ag^+ with (**C**) different

View Article Online
DOI: 10.1039/C7GC00503B

water mole fractions and (**D**) different kinds of promoters (a: 5 mM; b: 10 mM; c: 20 mM; d: 30 mM).

We investigated the effect the water mole fraction in the electrolyte on the electrochemical reaction using **Cu 1**/BN-C_{30} electrode (Fig. 2C). The current density and Faradaic efficiency of acetic acid were highest when the electrolyte contained 25 mol% [Emim]BF_4 and 75 mol% water. Both current density and Faradaic efficiency of acetic acid increased dramatically with increasing water concentration at the beginning, but decreased after water mole fraction exceeded 75 mol%. IL can play a catalytic role on the stabilization of radical species such as $CO_2^{\cdot-}$ [35] and the addition of water can affect the electrolysis in two opposite ways.[23] The viscosity of [Emim]BF_4 decreases with the addition of water, which enhances the conductivity. On the other hand, the number of ionic species in the electrolyte decreases with increasing IL concentration. The attained highest rate can be also attributed to the high concentration of H^+ in the electrolyte (Table S5). It has been demonstrated that the adsorbed CO (CO_{ads}), CHO (CHO_{ads}) and CH_3O (CH_3O_{ads}) for protonation and the C-C path for dimerization are strongly pH-dependent over Cu-based electrode, which may be attributable to reduce the free energy barrier of these processes.[36] Meanwhile, low pH can depress the HER and enhance the Faradaic efficiency of CO_2 reduction.[36]

The effect of inorganic salt LiI was also important for producing acetic acid. It was found that no acetic acid was formed without LiI (Fig. S17). When other inorganic salts in Fig. 2D were utilized, the Faradaic efficiency of acetic acid was poor. LiI was the best promoter in catalytic CO_2 reduction to acetic acid. The proper ion size and stronger Lewis acidity of Li^+may be favorable to producing acetic acid.[37] Moreover, the strong nucleophilicity of I^- can facilitate the formation of C-C bond in CO_2 reduction to acetic acid.[29]

We determined the electrokinetic data in order to studythe mechanism of CO_2 reduction to acetic acid. The equilibrium potential for acetic acid generation was -1.68 V vs Ag/Ag^+, which was obtained from extrapolation method[38,39] using the current densities for acetic acid at different potentials (Fig. S18). Therefore, the overpotential for acetic acid can be easily calculated, and was 0.52 V for this process at -2.2 V vs Ag/Ag^+ with the current density of 13.9 mA·cm^{-2}, which was very low for acetic acid production. Tafel plots in Fig. 3A show the variation of overpotential versus the partial current density for acetic acid production over **Cu 1**/BN-C_{30} electrode. The plot is linear in the overpotential rangefrom 0.12 to 0.30 V with a slope of 102.7 mV dec^{-1} for **Cu 1**/BN-C_{30} electrode, indicating that single electron transfer to CO_2 to form adsorbed $CO_2^{\cdot-}$ intermediate is a pre-equilibrium prior to a rate-determining step for our system.[40] The main product is acetic acid rather than formic acid, suggesting that the C-C coupling is faster than the protonation of $CO_2^{\cdot-}$.

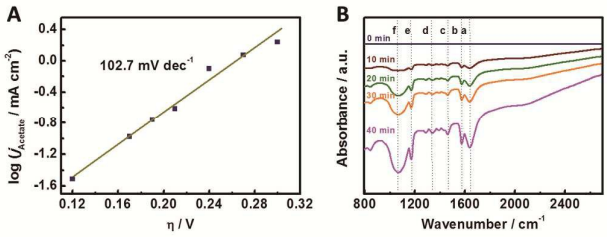

Fig. 3 A) Tafel plot for acetic acid production over **Cu 1**/BN-C_{30} electrode in [Emim]BF_4 aqueous solution with 25 mol% [Emim]BF_4 and 75 mol% water, in the presence of 0.01 M LiI. **B)** IR spectra of the electrolyte phase in above system at different electrolysis times and -2.2 V vs Ag/Ag^+.

Fig. 3B presents the electrolysis time-dependent infrared (IR) spectra for CO_2 reduction over **Cu 1**/BN-C_{30} electrode in [Emim]BF_4 aqueous solution with 25 mol% [Emim]BF_4 and 75 mol% water, in the presence of 0.01 M LiI at -2.2 V vs Ag/Ag^+. The signal of the original CO_2-saturated electrolyte was used as the background, and no peak can be observed from IR spectra before electrolysis started. After electrolysis started, the formation of COO^- can be verified from the peaks at 1639 (a) and 1331 cm^{-1} (d).[11,41] The intensity increased with the increasing electrolysis time. The peak at 1576 cm^{-1} (b) was attributed to the acetic acid dimer.[41] They indicate the formation of acetic acid along with theappearance of CH_3 peak at 1466 cm^{-1} (c). In addition, the bands related to C–H and C–O areobserved at 1172 (e) and 1061 cm^{-1} (f), respectively.

The high performance of **Cu 1**/BN-C_{30} electrode for CO_2 reduction to acetic acidis probably related to the synergistic effect between Cu complexes and BN-C_{30}. It is worth noting that BN-C_{30} can generate large amounts of formic acid and bulk BN has no CO_2 reduction product. N-doped graphitic carbon materials can adsorb CO_2 and stabilize $CO_2^{\cdot-}$.[19,23] N can induce some defect sites and polarize the adjacent C atoms.[19] The resulted positively charged C atoms and defects can facilitate the formation of $CO_2^{\cdot-}$. On the other hand, Cu (I)-based materials are able to bind $CO_2^{\cdot-}$ and CO_{ads} intermediate strongly for the further conversion to multi-carbon products.[12-14] Fig.S19 compares the performance of **Cu 1**/BN-C_{30} electrode with CuI/BN-C_{30} electrode, Tppda ligand/BN-C_{30} electrode and CuI+Tppda ligand (physical mixture of CuI and Tppda ligand)/BN-C_{30} electrode. It can be found that no acetic acid can be obtained over CuI/BN-C_{30} electrode and Tppda ligand/BN-C_{30} electrode. A very little amount of acetic acid can be obtained over CuI+Tppda ligand/BN-C_{30} electrode.So the coupling effect of Cu (I) center and N-based ligand in the complex **Cu 1** can help the bonding of CO_{ads}. It favors the further reduction of CO to methanol and C-C coupling for the acetic acid formation in the present of LiI. This pathway is also supported by the fact that acetic acid was not formed without LiI (Fig. S17). As mentioned above, the potential has significant impact on the selectivity of CO_2 reduction. For C-C coupling, two C-based adsorbates must be adjacent to one another and relatively favourable reaction energetics may be needed. In the meantime, the proton and electron transfer becomes

View Article Online
DOI: 10.1039/C7GC00503B

easier at more negative potentials. Therefore, the high activity of **Cu 1**/BN-C_{30} electrode for CO_2 reduction to acetic acid can be attributed to the synergistic effect among the C-doped BN, Cu metal center, N-based ligand, and the electrolyte.

On the basis of all the results above, we proposed a plausible mechanism for electrocatalytic CO_2 reduction to acetic acid (Fig. 4). First, CO_2 is adsorbed on the surface of electrode and reduced to $CO_2^{\cdot-}$ in the present of [Emim]BF_4, which may be due to that the complex [Emim-CO_2]$^+$ formed through the hydrogen bond between CO_2 and [Emim]$^+$.[42,43] It can reduce the reaction barrier forelectron transfer to CO_2.[35,44] Then, the formation of CO_{ads} and the protonation of $CO_2^{\cdot-}$ may occur simultaneously, and the former is the main procedure. CO_{ads} can be transformed into CHO_{ads} *via* capturing a pair of electron and proton, followed by the protonation of CHO_{ads}, which formed CH_3O_{ads} *via* accepting another two electrons. The downstream step is the conversion of CH_3O_{ads} to methanol, which was detected in the product. Subsequently, with the promotion of Lewis acidic cation Li^+, CH_3I may form on the surface of electrode by the reaction of methanol and I^-. It can be captured by the Cu species (Cu*) to form CH_3Cu*I, which is a basic step in organic synthesis and has been well proven.[29,37] As the process of $CO_2^{\cdot-}$ formation *via* single electron transfer to CO_2 is fast, CH_3Cu*I can combine with another $CO_2^{\cdot-}$ and generate CH_3COOCu*I. Finally, CH_2COOCu*I is protonated, resulting in the production of acetic acid. The by-products, LiOH and HI generated *in situ* neutralized spontaneously to form LiI and H_2O. All these catalytic species can be regenerated for the next process. Discussion of more detailed mechanism is very interesting, but is very difficult at present, which needs to be studied further.

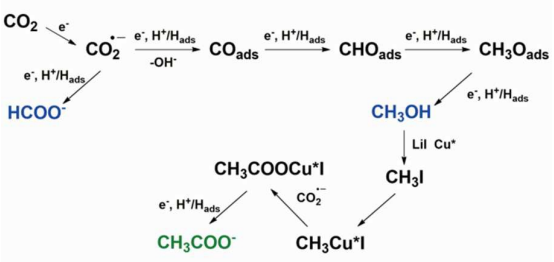

Fig. 4 Schematic pathway for electrocatalytic CO_2 reduction to acetic acid in this work.

Conclusions

In conclusion, we have discovered that **Cu 1**/BN-C_{30} exhibits the highest performance for electrochemical reduction of CO_2 to acetic acid up to date. The Faradaic efficiency of acetic acid can reach 80.3 % at a current density of 13.9 mA cm^{-2} in [Emim]BF_4 aqueous solution with 25 mol% [Emim]BF_4 and 75 mol% water in the presence of 0.01 M LiI. The superior performance of **Cu 1**/BN-C_{30} results mainly from the synergistic effect among the BN-C_{30}, Cu metal center, N-based ligand, and the electrolyte for producing acetic acid. BN-C_{30} can adsorb CO_2 and convert it to $CO_2^{\cdot-}$. Cu complex can help the formation and protonation of CO_{ads}, CHO_{ads} and CH_3O_{ads},and the C-C coupling in the presence of LiI. This study opens a way for highly efficient CO_2 reduction to C_2+ products by combination of composite catalysts and suitable electrolytes with promoter.

Acknowledgements

The authors thank the National Natural Science Foundation of China (21133009, 21533011, 21403253) and Chinese Academy of Sciences (QYZDY-SSW-SLH013).

Notes and references

1 J. Klankermayer, S. Wesselbaum, K. Beydoun and W. Leitner, *Angew. Chem. Int. Ed.*, 2016, **55**, 7296.
2 E. M. Nichols, J. J. Gallagher, C. Liu, Y. Su, J. Resasco, Y. Yu, Y. Sun, P. Yang, M. C. Y. Chang and C. J. Chang, *Proc. Natl. Acad. Sci. U. S. A.*, 2015, **112**, 11461.
3 M. He, Y. Sun and B. Han, *Angew. Chem. Int. Ed.*, 2013, **52**, 9620.
4 M. Aresta, A. Dibenedetto and A. Angelini, *Chem. Rev.*, 2014, **114**, 1709.
5 M. Cui, Q. Qian, Z. He, Z. Zhang, J. Ma, T. Wu, G. Yang and B. Han, *Chem. Sci.*, 2016, **7**, 5200.
6 L. Zhang and Z. Hou, *Chem. Sci.*, 2013, **4**, 3395.
7 D. D. Zhu, J. L. Liu and S. Z. Qiao, *Adv. Mater.*, 2016, **28**, 3423.
8 J. Qiao, Y. Liu, F. Hong and J. Zhang, *Chem. Soc. Rev.*, 2014, **43**, 631.
9 C. E. Tornow, M. R. Thorson, S. Ma, A. A. Gewirth and P. J. A. Kenis, *J. Am. Chem. Soc.*, 2012, **134**, 19520.
10 F. Calle-Vallejo and M. T. M. Koper, *Angew. Chem. Int. Ed.*, 2013, **52**, 7282.
11 Y. Liu, S. Chen, X. Quan and H. Yu, *J. Am. Chem. Soc.*, 2015, **137**, 11631.
12 D. Ren, Y. Deng, A. D. Handoko, C. S. Chen, S. Malkhandi and B. S. Yeo, *ACS Catal.*, 2015, **5**, 2814.
13 F. S. Roberts, K. P. Kuhl and A. Nilsson, *Angew. Chem. Int. Ed.*, 2015, **54**, 5179.
14 C. W. Li and M. W. Kanan, *J. Am. Chem. Soc.*, 2012, **134**, 7231.
15 R. Angamuthu, P. Byers, M. Lutz, A. L. Spek and E. Bouwman, *Science*, 2010, **327**, 313.
16 S. Lee, D. Kim and J. Lee, *Angew. Chem. Int. Ed.*, 2015, **54**, 14701.
17 A. A. Peterson, F. Abild-Pedersen, F. Studt, J. Rossmeisl and J. K. Norskov, *Energy Environ. Sci.*, 2010, **3**, 1311.
18 K. J. P. Schouten, Y. Kwon, C. J. M. van der Ham, Z. Qin and M. T. M. Koper, *Chem. Sci.*, 2011, **2**, 1902.
19 B. Kumar, M. Asadi, D. Pisasale, S. Sinha-Ray, B. A. Rosen, R. Haasch, J. Abiade, A. L. Yarin and A. Salehi-Khojin, *Nat. Commun.*, 2013, **4**, 2819.
20 C. W. Machan, S. A. Chabolla, J. Yin, M. K. Gilson, F. A. Tezcan and C. P. Kubiak, *J. Am. Chem. Soc.*, 2014, **136**, 14598.
21 S. Zhang, P. Kang, S. Ubnoske, M. K. Brennaman, N. Song, R. L. House, J. T. Glass and T. J. Meyer, *J. Am. Chem. Soc.*, 2014, **136**, 7845.
22 A. S. Varela, N. Ranjbar Sahraie, J. Steinberg, W. Ju, H.S. Oh and P. Strasser, *Angew. Chem. Int. Ed.*, 2015, **54**, 10758.
23 X. Sun, X. Kang, Q. Zhu, J. Ma, G. Yang, Z. Liu and B. Han, *Chem. Sci.*, 2016, **7**, 2883.
24 M. Xu, T. Liang, M. Shi and H. Chen, *Chem. Rev.*, 2013, **113**, 3766.
25 L. M. Azofra, D. R. MacFarlane and C. Sun, *Chem. Commun.*, 2016, **52**, 3548.
26 Q. Sun, Z. Li, D. J. Searles, Y. Chen, G. Lu and A. Du, *J. Am. Chem. Soc.*, 2013, **135**, 8246.

View Article Online
DOI: 10.1039/C7GC00503B

27 H. Guo, W. Zhang, N. Lu, Z. Zhuo, X. C. Zeng, X. Wu and J. Yang, *J. Phys. Chem. C*, 2015, **119**, 6912.
28 R. A. Periana, O. Mironov, D. Taube, G. Bhalla and C. J. Jones, *Science*, 2003, **301**, 814.
29 Q. Qian, J. Zhang, M. Cui and B. Han, *Nat. Commun.*, 2016, **7**, 11481.
30 K. J. Wei, Y. S. Xie, J. Ni, M. Zhang, Q. L. Liu, *Cryst. Growth Des.,* 2006, **6**, 1341.
31 J. Ni, K. J. Wei, Y. Z. Min, Y. W. Chen, S. Z. Zhan, D. Li, Y. Z. Liu, *Dalton Trans.,* 2012, **41**, 5280.
32 W. Yang, L. Chen, S. Wang, *Inorg. Chem.,* 2001, **40**, 507.
33 C. Huang, C. Chen, M. Zhang, L. Lin, X. Ye, S. Lin, M. Antonietti and X. Wang, *Nat. Commun.*, 2015, **6**, 8698.
34 Y. Shi, C. Hamsen, X. Jia, K. K. Kim, A. Reina, M. Hofmann, A. L. Hsu, K. Zhang, H. Li, Z.Y. Juang, M. S. Dresselhaus, L. J. Li and J. Kong, *Nano Lett.*, 2010, **10**, 4134.
35 B. A. Rosen, A. Salehi-Khojin, M. R. Thorson, W. Zhu, D. T. Whipple, P. J. A. Kenis and R. I. Masel, *Science*, 2011, **334**, 643.
36 H. Xiao, T. Cheng, W. A. Goddard and R. Sundararaman, *J. Am. Chem. Soc.*, 2016, **138**, 483.
37 Y. Oh and X. Hu, *Chem. Soc. Rev.*, 2013, **42**, 2253.
38 C. Costentin, G. Passard and J. M. Saveant, *J. Am. Chem. Soc.*, 2015, **137**, 5461.
39 Q. Zhu, J. Ma, X. Kang, X. Sun, H. Liu, J. Hu, Z. Liu and B. Han, *Angew. Chem. Int. Ed.*, 2016, **55**, 9012.
40 Y. Chen, C. W. Li and M. W. Kanan, *J. Am. Chem. Soc.*, 2012, **134**, 19969.
41 M. Gadermann, D. Vollmar and R. Signorell, *Phys. Chem. Chem. Phys.*, 2007, **9**, 4535.
42 P. Zhang, T. Wu and B. Han, *Adv. Mater.*, 2014, **26**, 6810.
43 X. Kang, X. Sun and B. Han, *Adv. Mater.*, 2016, **28**, 1011.
44 X. Sun, Q. Zhu, X. Kang, H. Liu, Q. Qian, Z. Zhang and B. Han, *Angew. Chem. Int. Ed.*, 2016, **55**, 6771.

View Article Online
DOI: 10.1039/C7GC00503B

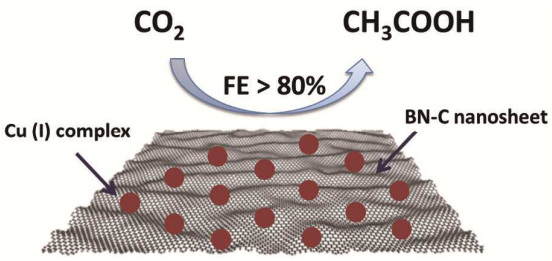

Cu (I) complex/BN-C_x composites exhibited high performance for electrochemical reduction of CO_2 to acetic acid in [Emim]BF_4-LiI-water electrolyte.